Assessment of in-service stresses in steel bridges for high-frequency mechanical impact applications

Engineering Structures 241 (2021) 112498

Contents lists available at ScienceDirect

Engineering Structures

journal homepage: www.elsevier.com/locate/engstruct

Assessment of in-service stresses in steel bridges for high-frequency mechanical impact applications

Poja Shams-Hakimi [b], Fredrik Carlsson [b], Mohammad Al-Emrani [a], Hassan Al-Karawi [a,*]

[a] Chalmers University of Technology, Sweden
[b] WSP Sweden AB, Sweden

ARTICLE INFO

Keywords:
Fatigue
Bridge
Traffic
HFMI
Variable amplitude
Mean stress
Overload

ABSTRACT

The application of high-frequency mechanical impact (HFMI) treatment to improve the fatigue performance of composite steel and concrete road bridges was studied through a state-of-the-art review in conjunction with simulations of variable amplitude in-service stresses in four case-study bridges in Sweden. Empirical stress range spectra with associated mean stresses were characterised for HFMI-treated bridges. It was shown that the fatigue-critical locations in HFMI-treated bridges remain unchanged compared with conventional bridges and that compressive overloads pose no detrimental effect that requires additional attention in the fatigue assessment. Calculations also showed a considerably better fatigue performance if HFMI treatment is performed on site, after the application of self-weight stresses.

1. Introduction

Bridges are designed for service lives of 80–120 years, which makes fatigue failure at the weldments a dominant design criterion. To prevent fatigue failure at the weldments, increased plate dimensions are commonly used along large parts of a bridge. As a result, an optimised lightweight design is inhibited and the use of high-strength steels becomes irrelevant. Improving the fatigue strength of bridges at some critical locations can result in considerable material saving, especially in conjunction with increased steel grades.

High-frequency mechanical impact (HFMI) treatment, which mainly improves fatigue strength by inducing local compressive residual stresses at the weld toe, can be suitable for improving the fatigue strength of bridge welds, particularly since it has been proven to perform well in the high-cycle regime. However, the implementation of HFMI treatment on bridges entails additional considerations which do not normally need to be taken into account in the fatigue design of conventional welds (as-welded joints). For as-welded (AW) joints in bridges, the nominal mean stress is thought to have no influence on fatigue life, as high tensile residual stresses are presumed locally at the weld toe. Nor are rarely occurring overloads a matter of concern, since their contribution to damage is low and they cause favourable relaxation of the tensile residual stresses from welding due to local yielding. For HFMI-treated welds, on the other hand, tensile mean stresses may substantially reduce the degree of improvement and overloads, if they result in significant local yielding at the weld toe, can partially or fully relax the compressive residual stresses [1].

The aim of this paper is to study realistic in-service stresses in composite steel and concrete road bridges with the emphasis on mean stress and overloads for the application of HFMI treatment. Composite steel and concrete road bridges are of special interest for HFMI investigation for two principal reasons. Firstly, due to the heavy concrete deck, self-weight stresses are high in relation to the stresses generated by traffic, causing an adverse mean stress effect. Secondly, as opposed to railway traffic, for example, there is large variability in the load effects from road traffic which can result in unfavourable overload stresses that are difficult to predict. This variability stems from traffic composition, such as truck weights and the lengths and presence of overloaded trucks, as well as from traffic positions in the transverse direction of bridges and traffic interaction. Traffic interaction includes meetings between trucks and trucks in caravans on bridges. Numerous research studies covering the topics of highway traffic loads [2–7], in-service stresses [8–11] and fatigue assessment related to steel bridges [12–18] are available in the literature. Some studies of HFMI treatment in bridge contexts are also available [19–22]. However, there are still scarcity in the number of studies that evaluate realistic load effects in bridges with emphasis on HFMI treatment [23–27].

In this paper, the in-service stresses of four case-study bridges were simulated using traffic data measured on Swedish roads. The application

* Corresponding author at: Chalmers University of Technology, Sweden.
E-mail addresses: poja.shams@wsp.com (P. Shams-Hakimi), Mohammad.Al-Emrani@chalmers.se (M. Al-Emrani), hassan.alkarawi@chalmers.se (H. Al-Karawi).

https://doi.org/10.1016/j.engstruct.2021.112498
Received 17 March 2021; Accepted 2 May 2021
Available online 12 May 2021

Nomenclature

AW	as-welded
CA	constant amplitude
CC	compression-compression
FAT	fatigue strength at two million cycles
HFMI	high-frequency mechanical impact
TC	tension-compression
TT	tension-tension
VA	variable amplitude
D	damage factor
f_u	ultimate tensile strength
f_y	yield stress
k	slope of the stress range vs. mean stress relationship
K_n	stress concentration factor (effective notch stress)
R	stress ratio
S	nominal stress
γ	safety factor
η	scaling coefficient on nominal stresses

of HFMI treatment on these bridges was then evaluated based on a state-of-the-art review with regard to the effects of overloads and variable amplitude (VA) loading on the fatigue strength of HFMI-treated welds. An experimental investigation of this topic, including VA fatigue testing, will be presented in a future publication.

Previous work has clearly shown that the effect of compressive overloads is more detrimental than that of tensile ones. Moreover, several existing studies of VA loading have shown that lower fatigue strength should be expected compared with constant amplitude loading. These studies included specimens with longitudinal attachment joints which commonly have high stress concentrations at the weld toe. The detrimental effect of VA loading was attributed to the relaxation of the beneficial residual stresses. On the other hand, studies of transverse attachment joints did not confirm any clear detrimental effect of VA loading.

The investigation of the case-study bridges in this paper revealed a number of principal differences between the in-service stresses and the types of VA load that have been used in most available experimental studies of HFMI-treated joints. The most prominent difference is that the mean stresses are high and the stress ranges relatively low, which results in very high stress ratios in the spectra of composite steel and concrete road bridges. Moreover, the mean stresses fluctuate in damage-critical locations. Although most stress cycles have very small ranges, a small percentage have exceptionally large ranges. This results in equivalent stress ranges that are much smaller than the maximum stress ranges in the spectra and spectrum shapes which might not be adequately modelled by theoretical probability density functions. Further observations were that compressive stresses appear in low-damage regions and are associated with low overall mean stresses. As a result, the consequence of reduced fatigue strength due to compressive overloads is minor.

2. State of the art

2.1. The effect of overloads

In this paper, the term “overload” is used qualitatively to describe stress cycles with exceptionally high peaks, either tensile or compressive, that might cause quasi-static relaxation of the beneficial residual stresses at the weld toe and impair the fatigue strength of HFMI-treated joints. It is believed that the quasi-static relaxation of residual stresses only occurs once for a large cycle and not again if the peak stress of that cycle is not exceeded, see Tai and Miki [25] or Mikkola et al. [28], for example. On the other hand, residual stress relaxation due to cyclic loading (with no overloads) is a progressive process and the rate of relaxation depends on the magnitude and mean value of the load, as shown by Dalaei et al. [29] and Shimanuki and Tanaka [30], for example. Residual stress relaxation due to cyclic loading is, however, outside the scope of this paper. Instead, this section focuses on the effect of a few overloads (preloads) prior to the constant amplitude (CA) fatigue testing of HFMI-treated welds.

For transverse butt welds, Ummenhofer et al. [31] observed no influence by compressive or tensile preloads on the state of residual stresses in HFMI-treated joints. With reference to fatigue strength, tensile preloads resulted in increased strength, which was believed to stem from the straightening of distortions, which reduced secondary bending stresses. Compressive preloads did not change the fatigue strength. The preloads in both tensile and compressive directions were equal to a nominal stress of $S_{prel} = 1.0f_y$.

For longitudinal attachments, Deguchi et al. observed no effect by tensile preloads of $S_{prel} = 1.0f_y$ on fatigue strength [32]. A stress ratio of $R = 0$ was used. On the other hand, it was shown that compressive preloads of $S_{prel} = -1.0f_y$ clearly removed the benefit of HFMI treatment. This was supported by Ishikawa et al. [33], where compressive preloads with nominal stresses of $S_{prel} \leq -0.68f_y$ were shown to remove the benefit of HFMI treatment. Compressive preloads of $S_{prel} \geq -0.46f_y$ did not change the fatigue strength notably compared with non-preloaded HFMI-treated specimens. The stress ratio was $R = -1$ in this study.

Martinez and Haagensen [34] tested transverse attachment joints under $R = 0.1$ bending with five compressive preloads of $S_{prel} = -0.85f_y$. A characteristic fatigue strength of FAT 151 was obtained. For joints like this under axial loading, the Eurocode provides FAT 80 [35] for the AW state. In the experiments by Okawa et al. [36] on transverse attachments, a preload of $0.9f_y$ in tension resulted in a reduction in fatigue strength and residual stress relaxation similar to that of a preload of $-0.6f_y$ in compression. A steel grade with $f_y = 520$ MPa was used in this study and measurements showed that the surface residual stresses relaxed from −400 to −250 MPa closest to the weld toe due to preloading. In spite of this, a significant fatigue strength improvement was obtained compared with AW specimens without preloads; FAT 206 compared with FAT 87 in mean strength, under $R = 0.1$ loading. Polezhayeva et al. [37] performed fatigue tests with various levels of compressive preload on transverse attachment joints, showing a gradual decrease in fatigue strength for preloads of $-0.46f_y$, $-0.53f_y$, $-0.62f_y$ and $-0.71f_y$, under $R = 0.02$ loading. All the results were still equal to or above FAT 160. In addition, Polezhayeva et al. [37] revealed that compressive preloads of $-0.71f_y$ actually relaxed all the compressive residual stresses from −350 MPa and introduced +400 MPa tensile residual stresses ($f_y = 560$ MPa). Nevertheless, the fatigue lives were still improved by a factor of 3–6, even with that level of preload.

2.1.1. Conclusions from the overload studies

The main findings from previous studies of the effect of initial overloads (preloads) on the fatigue strength of HFMI-treated joints are summarised below. The results from the available fatigue tests are also evaluated by the authors in view of the recommendations of the International Institute of Welding (IIW) [38].

With reference to tensile preloads, the reviewed studies included butt welds [31] ($S_{prel} = 1.0f_y$), longitudinal attachments [32] ($S_{prel} = 1.0f_y$) and transverse attachments [36] ($S_{prel} = 0.9f_y$). Only one study reported a decrease in fatigue strength [36]. Nevertheless, all the results conformed conservatively to the characteristic *SN* curves for HFMI-treated joints provided by the IIW.

In terms of compressive preloads, only longitudinal attachment specimens with very large compressive preloads of $S_{prel} \leq -0.68f_y$ [32,33] exhibited fatigue lives below the characteristic IIW *SN* curves. This was most probably due the high stress concentration at the weld toe in these weldments compared with butt welds and transverse attachments. Longitudinal attachment specimens preloaded to $S_{prel} \geq -0.46f_y$

still conformed to the IIW *SN* curves. However, it should be noted that the CA testing following the preloads was performed at $R = -1$ in [33]. If a higher stress ratio (e.g. $R = 0.1$) had been used, the IIW *SN* curves might not have been conservative. For transverse attachment specimens, compressive preloads resulted in a reduction in fatigue strength in [36] ($S_{prel} = -0.6f_y$) and [37] ($-0.71 \leq S_{prel} \leq -0.46f_y$) but with results still above the IIW *SN* curves. No influence of compressive preloads could be observed for butt welds [31] ($S_{prel} = -1.0f_y$). These observations clearly show that an accurate estimation of the effect of preloads should take account of the stress concentration in the weldment. Moreover, it can be concluded that no result fell below the fatigue strength recommendations of the IIW for $-0.46f_y \leq S_{prel} \leq 1.0f_y$, irrespective of the type of weldment.

In Fig. 1, the fatigue results for the transverse and longitudinal attachment specimens were re-analysed with a fixed slope of $m = 5$ in terms of fatigue strength versus the degree of nominal stress preload (factor on f_y). Linear regression lines clearly show that the slope of the reduction in fatigue strength is steeper for compressive preloads than for tensile ones.

To conclude, compressive overload appears to be more detrimental than the tensile ones. Moreover, the IIW recommendation regarding overload limitations does not provide guidance for compressive overloads. However, the studies show that none of the HFMI-treated specimens has a fatigue strength less than the recommended values by the IIW even when preceded by compressive preloaded.

2.2. The effects of variable amplitude loading

This section presents a review of studies from the literature of the effects of variable amplitude (VA) loading on the fatigue resistance of HFMI-treated weldments. The studies included both general-purpose investigations and investigations oriented towards crane, offshore and bridge structures. Most of the reviewed studies included load cycles originating from spectra with theoretical probability density functions (PDFs) and cycle-by-cycle random sequences. A special case was studied by Leitner et al. [39] where random sequence spectrum loading was performed with $R = 0.1$ but for 1000 equal stress ranges at a time. The spectrum PDFs varied from being log linear, Gauss like (i.e. a convex shape with a greater number of large loads) or Weibull distributed (spectrum shape used for describing loads in bridges including overloads). Ghahremani et al. [24,27] performed experiments with random load cycle sequences based on empirical spectrum PDFs. The PDFs were based on simulations of bending moment and support reaction variations from traffic in two simply supported beam models and included varying stress ratios. Two studies included pure block loading [40,41] of a few stress magnitudes with $R = 0.1$, meaning that the loads did not originate from a specific spectrum and did not occur in a random sequence. Okawa et al. [36] studied block loading with a pattern describing storms, with a constant mean stress of 100 MPa.

Further differences between the studies were that 1) various omission strategies were used for the smallest stress ranges, 2) equivalent stress ranges were calculated using different methods; e.g. with single or bi-linear *SN* slopes based on either experimental constant amplitude (CA) fatigue test results or code *SN* curves. Similarly, 3) the calculated number of cycles to failure, N_{calc}, for the real cumulative damage sums ($D_{real} = N_{exp}/N_{calc}$) were obtained using different approaches. Besides, the studies were conducted on variety of steel qualities. A short overview of the studies is given in Table 1.

2.2.1. Conclusions from the variable amplitude studies

With the above-mentioned differences in mind, the following observations are made. Three studies including different spectrum PDFs (shapes) and mean stress properties indicated that the *SN* slope continues to be $m = 5$ in the high cycle regime. The longest fatigue lives

Table 1
Overview of the VA studies: T = transverse, L = longitudinal attachments.

Ref	Load type	Mean stress properties		Detail	f_y (MPa)
[25,26]	Spectrum: Weibull (bridge)	R = Varying	(fluctuating mean, only tension)	L	633
[24,27]	Spectrum: Empirical (bridge)	R = Varying	(fluctuating mean, only tension)	T	350
[36]	Block: Storm pattern (offshore)	R = Varying	(constant mean, 100 MPa including compression)	T	392
[42,43,44]	Spectrum: log linear/ Gauss like	R = −1	(constant mean, 0 MPa)	L	690
[45]	Spectrum: Gauss like (crane)	R = 0.1	(fluctuating mean)	T	1100
[39]	Spectrum: log-linear	R = 0.1	(fluctuating mean)	L	355–690
[40]	Block: case specific	R ≈ 0.1	(constant mean, $0.55*S_{max}$)	L	390
[41]	Block: case specific	R = 0.1	(fluctuating mean)	T	355–960

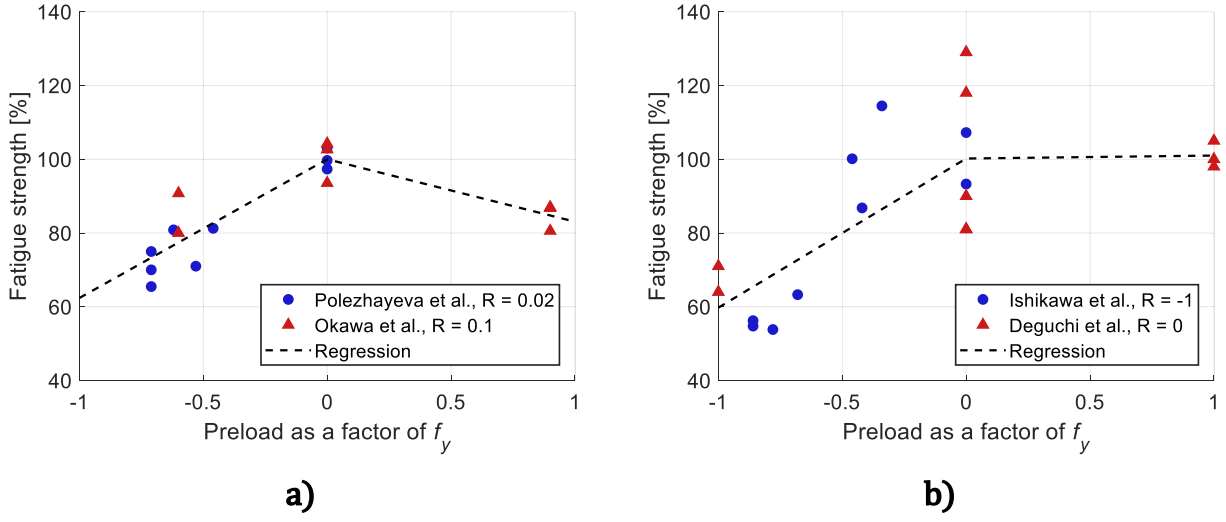

Fig. 1. Fatigue strength with a fixed slope of m = 5 of HFMI-treated transverse (a) and longitudinal (b) attachment specimens as a function of degree of preload.

were 70, 30 and 37 million cycles in [27,42,44], respectively.

The studies [25,27] which incorporated varying stress ratios (fluctuating mean) in spectrum loading both report a minor influence by the mean stress properties investigated. Tai and Miki [25] investigated two different loading patterns, both with an identical Weibull-distributed tension-tension spectrum, but, in one, the minimum stresses were kept constant, while, in the other, the maximum stresses were kept constant. The loading patterns were not thought to affect the fatigue lives significantly, although this was only based on four experimental results. Ghahremani et al. [27] tested two different load spectra from bridges with varying stress ratios, one containing mainly low stress ratios and the other containing mainly high stress ratios. Both spectra contained only tensile stresses and the minimum stress of the major cycles was seemingly constant and below 20 MPa. It was concluded that the stress ratio effect was not of crucial importance under spectrum loading. However, in [24], Ghahremani and Walbridge showed analytically that a tensile self-weight stress of 175 MPa almost removed the benefit of the HFMI treatment.

Although not investigating fluctuating mean stresses, Okawa et al. [36] compared the fatigue lives of transverse attachment joints under a storm load pattern with varying stress ratios, $-0.4 \leq R \leq 0.6$ (constant mean stress of 100 MPa). The lower stress ratios corresponded to the larger stress ranges. The worst storm loads were applied first so that potential residual stress relaxation would occur at the beginning of the testing. Only two HFMI-treated specimens were included, tested at different load levels; $\Delta S_{max} = 400$ and 500 MPa. For the specimen with the higher load level, the peak stresses were equal to $S_{max} = 0.89f_y$ and $S_{min} = -0.38f_y$. The HFMI specimens were both run-outs at 5.24 million cycles, whereas the AW specimens failed after 1.96 and 3.45 million cycles. This demonstrates considerable fatigue life enhancement, even in the presence of sizeable compressive stresses.

The real damage sum appears to be lower than 1.0 in several cases, indicating that the VA strength of HFMI-treated weldments is lower than the CA strength. By comparing bi-linear *SN* curves of VA and CA test results, Leitner et al. [39] suggested a reduced specific damage sum of 0.2–0.3 in order to avoid non-conservative predictions of the VA strength of HFMI-treated joints. However, re-evaluating the experimental results reveals that only one of the seven specimens had a real damage sum in the interval 0.2–0.3. Three specimens had damage sums between 0.7 and 0.9 and the rest were above 3.0, amounting to an average of 1.85. The tests included longitudinal attachments under $R = 0.1$ and applied maximum nominal stresses of $S_{max} = 0.94$–$1.56f_y$, depending on the specimen. To evaluate the degree of improvement under VA loading, Leitner et al. [39] compared Gassner curves which, instead of equivalent stress ranges, use the maximum stress range in the spectrum. This evaluation revealed almost no benefit of HFMI treatment. On the other hand, comparing *SN* curves based on equivalent stress ranges would have indicated a significant improvement by the HFMI treatment, with a 60% increase in fatigue strength at two million cycles. The characteristic strength of FAT 125 recommended by the IIW was shown to be highly conservative in relation to the test results. Huo et al. [40] performed fatigue tests with the block loading of longitudinal attachment specimens under $R = 0.1$ but with lower maximum nominal stresses, $S_{max} = 0.62$–$0.72f_y$. The real damage sums obtained were between 0.3 and 0.4, but a significant fatigue strength improvement of 80% at two million cycles was reported. All the HFMI results were above the FAT 140 curve, as recommended by the IIW for the specimens in question. Similarly, Yıldırım et al. [46] found real damage sums of 0.3–0.4 based on VA experiments from [43] of longitudinal attachments under $R = -1$ loading with a log-linear PDF. Two load levels with peak nominal stresses of $S_{max/\min} = \pm 0.54f_y$ and $\pm 0.70f_y$ were investigated. The FAT 160 curve recommended by the IIW was shown to be conservative with a notable margin, but almost all the AW results were also above this strength. The improvement factors were therefore comparably low. Tai and Miki [25] investigated VA bridge loads on longitudinal attachments, also showing very low real damage sums of $D \approx 0.2$. In spite of this, the results indicated a major improvement compared with AW joints, although no comparisons were made explicitly. Compared with the IIW, the results were located far above the recommended FAT 125 curve. Prior to spectrum loading, Tai and Miki subjected the specimens to one tensile overload almost equal to the maximum stress occurring in the spectrum. Despite the low maximum nominal stresses of $S_{max} = 0.43f_y$, significant residual stress relaxation was measured after the initial overload, from approximately -400 to -160 MPa, remaining relatively constant during the fatigue testing.

Some studies reported damage sums above 1.0. As different from the aforementioned studies which involved specimens with longitudinal attachments, these involved the fatigue testing of transverse attachment joints. Under block loading with $R = 0.1$, Leitner et al. [41] obtained a real damage sum of 1.6 for a maximum nominal stress of $S_{max} = 0.94f_y$ ($f_y = 355$ MPa). Interestingly, a yield stress dependence was observed where the real damage sums decreased as the steel grade increased; $D_{real} = 0.74$ for $S_{max} = 0.64f_y$ ($f_y = 690$ MPa) and $D_{real} = 0.63$ for $S_{max} = 0.46f_y$ ($f_y = 960$ MPa). On the other hand, Berg et al. [45] obtained real damage sums mostly lying above 2.0 for all the test results but one ($D_{real} = 0.8$) for $f_y = 1100$ MPa under Gauss like spectrum loading. Maximum nominal stresses of $S_{max} = 0.50$–$0.95f_y$ were used, depending on the specimen. Ghahremani et al. [27], oriented towards bridges, conducted high-cycle experiments and considered that a specified damage sum of 1.0 was appropriate for the calculation of equivalent stress ranges. A mean fatigue strength of FAT 202 with $m = 4.79$ was derived for the HFMI-treated VA specimens, which was of similar or higher fatigue strength than the CA test results and considerably higher than the AW VA results which had a mean strength of FAT 98 with $m = 2.79$. All the test results conformed conservatively to the IIW FAT 125 curve. The specimens were tested at maximum stresses of $S_{max} = 0.39$–$1.10f_y$.

In the context of VA loading, factors influencing failure mode have also been seen in several studies. Marquis and Björk [42] (also [47]) observed that the failure mode changed from the CA to the VA loading of longitudinal attachment joints ($R = -1$), going from various positions in CA loading always to toe failure in VA loading. This was believed to be caused by reduced fatigue strength at the weld toe due to the relaxation of the compressive residual stresses. Yildirim et al. [43] and Berg et al. [45] also showed load-level dependence of the failure modes, where toe cracking occurred almost only for higher load levels.

Several of the above studies ([40–42]) have already been included in a review by Nykänen et al. [48] with respect to the fatigue strength prediction of welded joints under VA loading. A new fatigue assessment method called the 3R method was utilised. It enabled consistent calculations and comparisons of real damage sums, including both AW and HFMI-treated joints. The damage sums obtained with the new assessment method were very similar to the values obtained conventionally using the nominal stress approach but tended to be less conservative. Furthermore, it should be mentioned that the studies in [40,42,43] were also reviewed by Mikkola et al. in [49]. Based on these studies and finite element simulations, Mikkola and Remes [50] considered that $S_{min} \geq -0.6f_y$ could be a suitable limit for compressive stresses to claim benefits from the HFMI treatment under $R = -1$ loading. The IIW currently limits compressive stresses to $-0.45f_y$ for $R = -1$ loading.

It can be concluded that variable amplitude loading (VA) has a significant detrimental effect on the fatigue strength of HFMI-treated joints. However, the obtained fatigue strength under VA loading conformed to the IIW fatigue strength. On the other hand, several studies show that treated transverse attachment tested under VA can be as good -if not better- as the ones tested under constant amplitude loading.

3. Method

The conducted literature study pinpoints the influence of load spectrum (variability and extreme load) on the efficiency of HFMI treatment. The examination of fatigue test results enables the use of IIW recommendation for analysing the in-service stresses in road bridges due

to variable truck loads. Moreover, the obtained knowledge about residual stress relaxation due to overload motivates investigating size of the maximum stresses in road bridges that may diminish the main beneficial effect of HFMI treatment.

In this paper, normal stresses from bending in four existing composite steel and concrete bridges have been studied by simulating the in-service response using truck loads from traffic measurements from Swedish roads. All the bridges comprised concrete decks in composite action with two steel girders. Fig. 2 shows the span lengths and Fig. 3 shows the bridge cross-sections and the expected transverse positions of traffic (one vertical arrow per traffic lane). Bridge 1 was too narrow to fit more than one lane and segments of Bridges 2 and 4 were designated for pedestrian traffic.

The bridges were all designed according to the Eurocodes and built in Sweden. Their original design calculations were collected from various consulting companies. For all the bridges, the fatigue limit state had utilisation ratios close to 1.0. The fatigue designs were performed using the Fatigue Load Model 3 (FLM3) in the Eurocode [51] and the damage equivalent factor method [52] (hereafter called the lambda method). A traffic intensity of 50,000 heavy trucks a year per slow lane was used in all designs. The safety factors of $\gamma_{Mf} = 1.35$ and $\gamma_{Ff} = 1.0$ were used on the resistance and load sides, respectively.

The traffic information used in this study has previously been published by Carlsson [2,53] and is the result of 87 days of measurements in total. In this current paper, a total of 55,000 unique trucks heavier than 100 kN (as suggested in [51]) were used, originating from 12 different locations in Sweden, including various types of road. It was shown by Carlsson that the mean truck lengths and mean truck weights were independent of the measurement location. The traffic composition in terms of vehicle types (i.e. number of axles) was also independent of the measurement location. Fig. 4 shows the truck weight (a) and weight-length distributions (b).

In order to simulate the in-service stresses, bending moment influence lines were created for different sections along each bridge with a spacing of ≤ 1 m, accounting for bending stiffness variations along the bridges. The bending stiffness variations originated from different steel girders and different effective widths of the concrete decks due to shear lag along the bridges, as well as cracking in the concrete deck over mid-supports. To account for dynamic effects, a dynamic amplification factor (DAF) of 1.2 was used for all the trucks, as suggested in Eurocode 1: Part 2 [51] for new bridges. Additionally, for bridge cross-sections within 6 m of the end supports, a linearly decreasing DAF from 1.3 to 1.0 was used to account for the dynamic effects of trucks passing over expansion joints. Furthermore, stresses from self-weight were calculated in each section in order to obtain realistic mean stresses, including the weights of the concrete deck, steel girders and pavement. The nominal stresses are evaluated along the bridge using beam theory, taking into consideration the effect of the concrete deck on both the load level (i.e. additional mean stresses) and the resistance level (i.e. additional bending stiffness).

The 55,000 trucks included in the load sequence were run over each influence line one by one and in a fixed transverse position on the bridges (centre of traffic lanes), resulting in deterministic stress-time histories. Subsequently, Rainflow counting according to [54] was performed on the stress-time histories to obtain stress cycles at each bridge cross-section. The effects of the simultaneous presence of trucks on the bridges and the variability in the transverse position were investigated separately from the deterministic results. The number of times that two heavy trucks are present on a bridge was calculated based on slow travel speeds of 30 km/h to obtain many occurrences of meetings and small vehicle distances in caravans. The approaches for calculating the number of occurrences were different for meetings and caravans and are both presented in [2]. For every occurrence of meeting/caravan, two trucks were randomly selected from the measurement data and the possibility of a truck meeting "itself" was allowed. To simulate the meetings, a meeting location was randomly selected on the bridge from a uniform probability distribution for each occurrence. The individual stress-time variations of the trucks were then superimposed with a certain time shift as a function of the meeting point. To simulate two trucks in a caravan, the distance between them was modelled as a random variable from a beta distribution, based on [2], resulting in a time shift between their individual stress-time variations which were then superimposed. The transverse traffic position was modelled as a random variable from a normal distribution with a mean at the centre of the traffic lanes and a standard deviation of 0.23 m [2].

4. Results

4.1. Effects of meetings, caravans and transverse position

The influence of simultaneous vehicles on fatigue damage was found to be negligible for the investigated bridges because the number of occurrences were simply too few. The variability of transverse traffic position resulted in increased damage factors of less than 1%. Due to the small influence, these aspects are disregarded from further evaluations of damage factors.

From the viewpoint of residual stress relaxation, it was of interest to investigate the size of maximum stresses that can occur due to these stochastic events. The presence of simultaneous trucks can, in rare, extreme cases, produce maximum stresses which are higher than those from single trucks. Likewise, there is a probability of heavy trucks travelling in an unfavourable transverse position. The severity of these extreme events depends on random variables such as the vehicles that are involved in the events, in case of meetings, the meeting location on

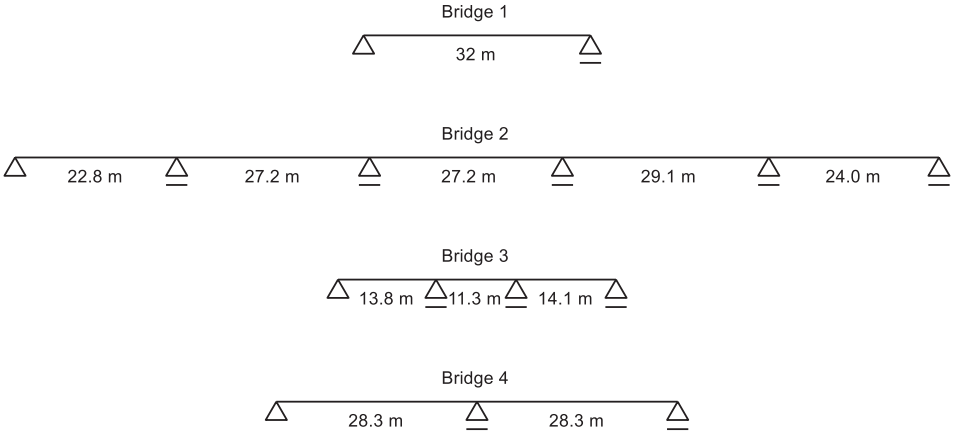

Fig. 2. Span lengths of the case-study bridges. All the bridges comprised composite concrete and steel systems with two I-beams.

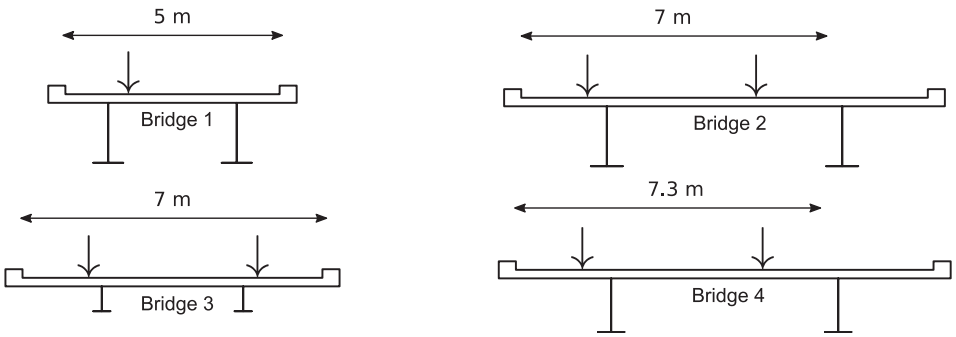

Fig. 3. The bridge cross-sections and expected traffic positions in the transverse direction. The vertical arrows represent the resultants of the traffic load in each lane.

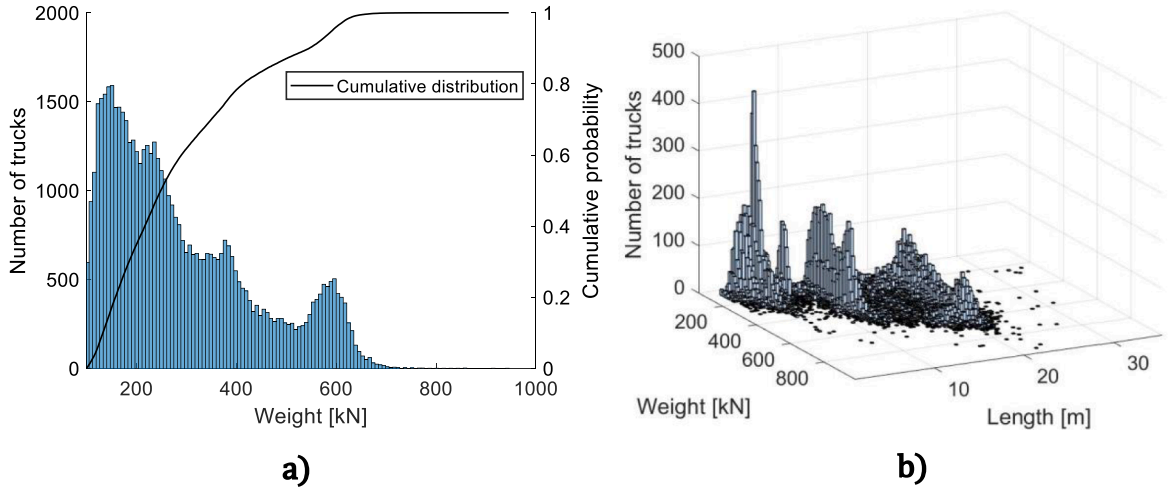

Fig. 4. Truck weight distribution (a) and weight-length distribution (b).

the bridge and, for caravans, the distance between the vehicles. To capture the effect of extreme events on maximum stress, the three event types were studied separately for the most critical bridge cross-sections using a number of Monte Carlo simulations corresponding to 100 times the design lives of the bridges. Since the bridges were subjected to low traffic intensities, 100 times their design lives was chosen in order to simulate a large number of events and consequently capture the more extreme ones. Since it is unlikely that the extreme events of meeting/caravans/transverse positions occur at the same time, only the largest effect of the three was considered. No investigation of the interaction of these events nor the likelihood of them occurring simultaneously was conducted.

4.2. As-welded bridges

A summary of damage factors and nominal stress results for as-welded (AW) bottom flange joints is given in Table 2, assuming FAT 80 along the whole bridges because it is the lowest FAT value among the existing details (i.e. 125 for flange-to web weld, 80 for transverse butt welds and cope holes) as shown in Fig. 5. This FAT class was also used in the original design calculations for the critical weldments. Both double- ($m = 3$ & 5) and single-slope ($m = 3$) equivalent stress ranges are presented, assuming specified damage of 1.0 with the expressions given by the IIW [55]. The damage factors were calculated using the Palmgren-Miner method with the bi-linear *SN* curves of Eurocode: Part 1–9 [35]. The slopes of 3 and 5 were used with slope transition at five million cycles and infinite life (cut-off limit) at >100 million cycles. The results in Table 2 refer to the sections with the greatest damage, which in all

Table 2
Results for bridge sections in the AW state with the greatest damage from measured traffic, $\gamma_{Mf} = 1.35$ and $\gamma_{Ff} = 1.0$. Values in parentheses refer to the effects of the most unfavourable extreme events. Stresses are nominal.

Bridge	Design life [Years]	Cycles above cut-off limit	S_{self} [MPa]	S_{max} [MPa]	ΔS_{max} [MPa]	ΔS_{eq3} [MPa]	$\Delta S_{eq3,5}$[MPa]	$D_{AW,orig}$[–]
1	80	3 300 000	123	241 (+10%)	117(+20%)	47	49	0.91
2	120	2 900 000	65	135 (+9%)	82 (+17%)	32	38	0.31
3	80	3 500 000	68	189 (+9%)	131(+14%)	41	43	0.62
4	80	3 500 000	112	216 (+10%)	127(+16%)	49	50	1.05

S_{self} – stress from self-weight.
S_{max} – highest stress peak in the load sequence including self-weight and traffic load.
ΔS_{max} – largest stress range in the load sequence.
ΔS_{eq3} – single-slope (m = 3) equivalent stress range.
$\Delta S_{eq3,5}$ – double-slope (m = 3 & 5) equivalent stress range assuming FAT 80.
$D_{AW,orig}$ – Damage in the original bridges with as-welded joints caused by the measured traffic.

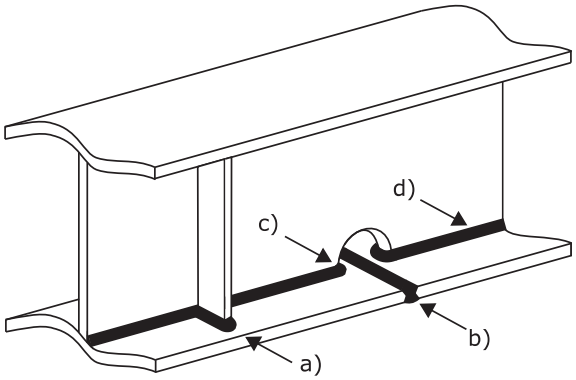

Fig. 5. Typical weldments in bridges; a) non-load-carrying transverse attachment, b) butt weld, c) cope hole and d) longitudinal flange-to-web weld.

cases occurred near the mid-spans. The damage factors in the top flanges were consistently smaller by a large margin and are therefore not tabulated. The maximum damage factors in the top flanges were 0.00, 0.14, 0.29 and 0.16 in the order of bridge number and occurred at the internal supports.

The damage factors obtained from the simulations were calculated with the same safety factors and traffic intensities as in the original fatigue design calculations. The fatigue design utilisation ratios from the original calculations were 0.89, 0.96, 0.89 and 0.98 in the order of bridge number (based on the lambda method). Comparing the design utilisation ratios with the calculated damage factors from measured traffic, $D_{AW,orig}$ in Table 2, the results for Bridges 1 and 4 were in good agreement. For Bridges 2 and 3, the differences were fairly large. The reason for this discrepancy is not clear, but it can be expected that the lambda method generates utilisation ratios with various degrees of conservatism from case to case. Based on these comparisons, it is considered that the simulation results are reasonable.

Fig. 6 shows the stress range spectra of the damage-critical sections, with both absolute (a) and normalised stress ranges (b). It is evident that Bridge 1 had the most unfavourable spectrum shape. The spectrum shapes were compared visually and tested statistically against a variety of theoretical probability density functions without fitting any of them (e.g. normal, log normal, Weibull, GEV etc.). The statistical tests were performed based on [56,57] at a 5% significance level.

The spectra in Fig. 6 apply to single truck passages and the fixed transverse position of traffic. It was observed in the study of the stochastic traffic events that the 50 largest cycles approximately (~0.1% of the total cycles in the sequence) were highly random, e.g. subject to significant change due to the stochastic events. For the damage-critical sections of Bridges 1 and 3, the variable transverse position of traffic gave rise to the largest increase in maximum stresses of 10% and 9%, respectively. For Bridges 2 and 4, meeting traffic had the worst effects on the maximum stress, 9% and 10%, respectively. These values from extreme events are given in parentheses in Table 2 and the corresponding effects on the maximum stress ranges are also tabulated.

It was interesting to compare the maximum stresses (which include stresses from self-weight) with the yield stresses of the original designs which were 400 (S420), 345 (S355), 335 (S355) and 400 MPa (S420) in the order of bridge number. The lower yield stresses compared with the nominal values account for the effect of thickness according to the EN-10025-2 standard. In Bridge 4, the section with the highest tensile stress did not coincide with the maximum damage section but was situated adjacent to it and contained a maximum stress of 223 MPa. So, accounting for extreme events, the ratios of maximum tensile stress to yield stress became 0.66, 0.43, 0.61 and 0.61. Moreover, the ratio of self-weight stress to maximum stress was 0.46, 0.44, 0.33 and 0.47. Another quantity of interest is the ratio of equivalent stress range to maximum stress range [58,59]. Using the double-slope equivalent stress ranges, these ratios became 0.35, 0.40, 0.29 and 0.34. Finally, from a design point of view, it was also relevant to compare the ratio of maximum stresses from measured traffic (excluding self-weight) to the maximum stresses generated by Eurocodes FLM 3 [51]. The measured traffic generated 2.3–2.4 times higher maximum stresses than FLM3.

4.3. Stress levels in HFMI-treated bridges

The goal of improving the fatigue strength of the most fatigue-critical weldments in a steel bridge is to reduce the use of steel to achieve a more optimised design. This, in turn, means that higher stresses from self-weight and stress ranges from traffic loads should be expected in a bridge with HFMI-treated weldments, due to a reduction in the moment of inertia, see Fig. 7. Every stress value in the load sequence (turning point) is elevated by the same proportion, η, when the bridge is optimised, and the same proportional increase also applies to every stress range in the spectrum. This assumes that the self-weight remains unchanged, which is a good estimation, since the self-weight is dominated to a large degree by the concrete deck.

In order to determine by how much the stresses will be elevated, the design limit state that will be governing for the optimised bridge must

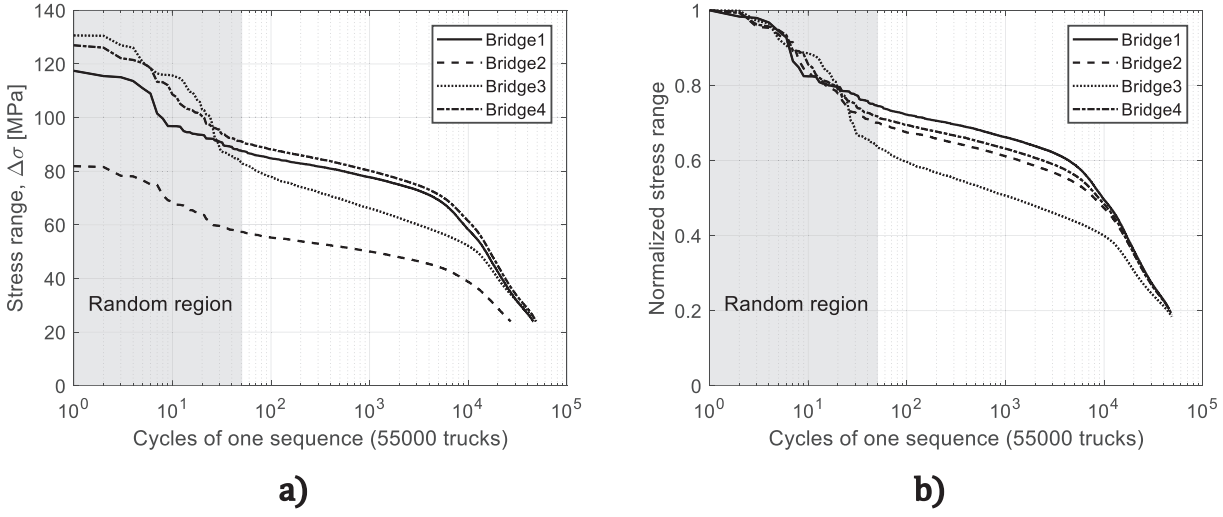

Fig. 6. Stress range spectra (cumulative frequency distributions) of the damage-critical sections. Only stress ranges above the cut-off limit for FAT 80 are included; a) includes absolute and b) normalised stress ranges.

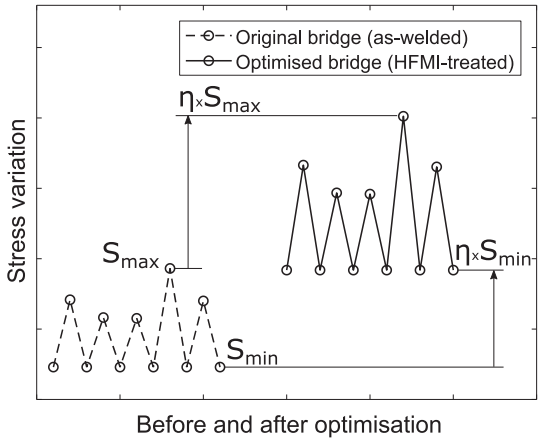

Fig. 7. Schematic illustration of the elevation of stresses by η in HFMI-treated bridges.

first be identified, which can be any of the following three; the ultimate, serviceability or fatigue limit state. However, the design of each bridge is unique, and the governing design limit state will depend on many aspects such as span lengths, girder dimensions, steel quality and so on. A maximum possible elevation of the stresses is therefore sought instead which is universally applicable to any bridge design. This can be determined by the fatigue strength of the longitudinal flange-to-web welds, see Fig. 5d. These welds are not expected to benefit from HFMI treatment as their fatigue strength is generally not determined by failure from the weld toe but rather by inner weld defects such as porosity, lack of fusion and so on. In [60], a study of the potential for material saving as a result of fatigue strength improvement was conducted; it included Bridges 1 and 2. It revealed that>20% steel could be saved before the fatigue limit state became limiting due to the flange-to-web welds. In other words, the ultimate and serviceability limit states did not limit the material saving of these bridges.

Depending on the welding method and other technical requirements, the flange-to-web welds can have a maximum fatigue strength of FAT 125 in the AW state according to both the Eurocode [35] and the International Institute of Welding [55]. It is recognised from the original design calculations of the four bridges that the fatigue-critical weldments in the AW condition are usually non-load-carrying transverse attachments, FAT 80, according to [35,55]. However, transverse butt welds and cope holes (Fig. 5) may also be present but in less critical locations. Since the fatigue-driving nominal stress for these weldments is the same stress which drives the fatigue of the flange-to-web welds, the maximum possible elevation of stresses can be set at $\eta = 125/80 = 1.56$. This provides the sought-after universal stress elevation for the optimised HFMI-treated bridges and will be used for further evaluations in this paper. Under adverse loading conditions, it is possible that the fatigue strength of the HFMI-treated weldments becomes lower than the strength of the flange-to-web welds. This is an additional reason for viewing the choice of $\eta = 1.56$ as the maximum possible elevation of stresses.

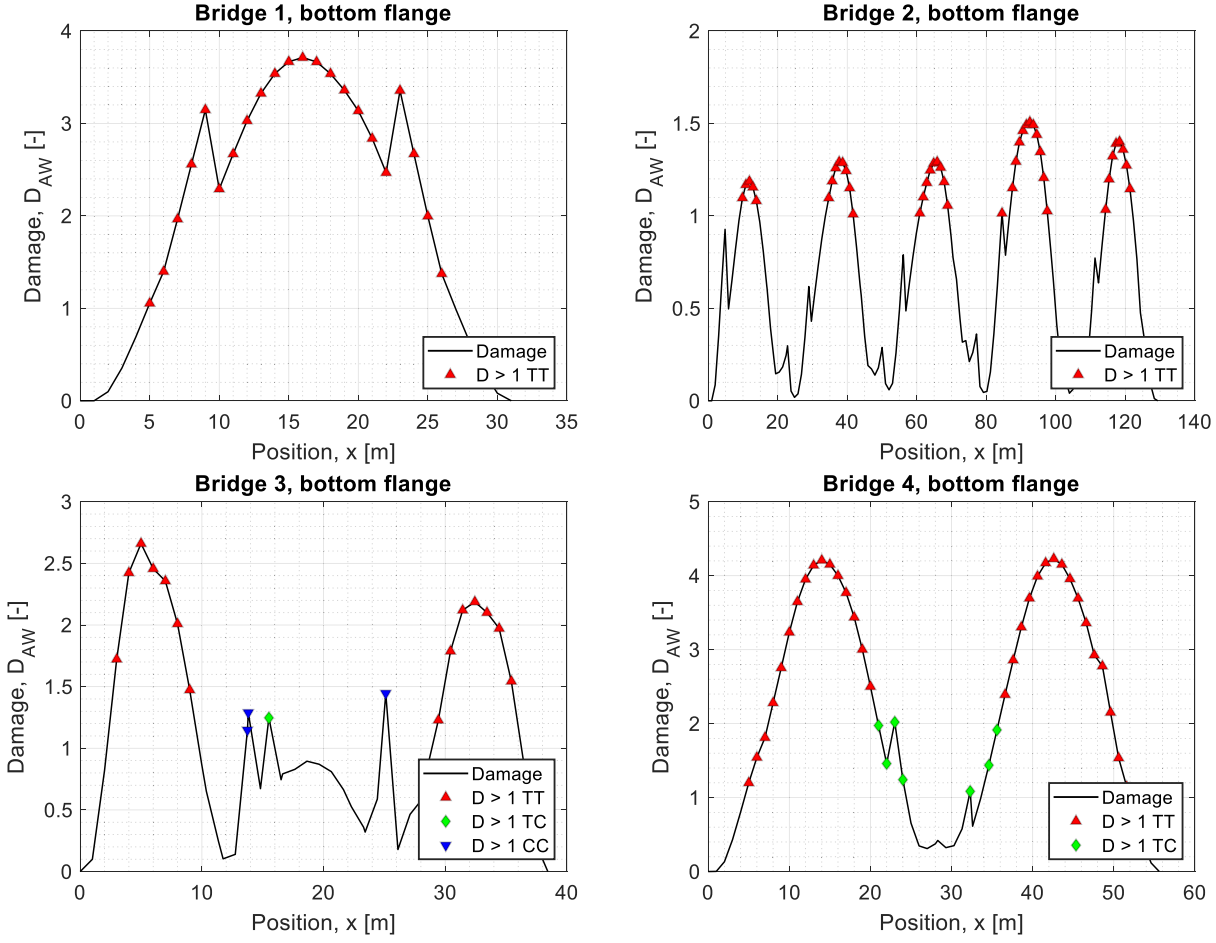

Fig. 8. Distinction of the optimised bridge sections requiring HFMI treatment ($D_{AW,opt} > 1.0$). AW (FAT 80) damage factors for stresses from measured traffic elevated by $\eta = 1.56$ ($\gamma_{Mf} = 1.35$ and $\gamma_{Ff} = 1.0$).

4.4. Bridge sections requiring HFMI treatment

To determine where along the optimised bridges HFMI treatment would be required, the elevation in stress of $\eta = 1.56$ was used together with the AW FAT 80 strength to distinguish cross-sections with AW damage factors ($D_{AW,opt}$) above 1.0, see Fig. 8. Since it was shown in the state-of-the-art review that compressive stresses are more detrimental in relaxing the beneficial compressive residual stresses, a further distinction of the bridge cross-sections was made by categorising them, depending on whether they experience solely tensile stresses (TT), tensile and compressive (TC) or solely compressive stresses (CC). It is evident from Fig. 8 that the most critical location for any weldment is near mid-spans where the sections only experience tensile stresses. Therefore, stresses from the most critical (TT) locations are studied first.

4.5. Bridge sections with only tensile stresses (TT)

In the following, stresses relevant to HFMI-treated bridge weldments are studied. Table 3 provides some characterising quantities for the critical sections for elevated stresses with $\eta = 1.56$. They represent the maximum expected stresses in the optimised bridges after HFMI treatment. Both double ($m = 5$ & 9) and single slope ($m = 5$) equivalent stress ranges are presented, assuming specified damage of 1.0 and FAT 140 (for $355 \leq f_y < 550$ MPa based on [38]). Here, the minimum stress range (ΔS_{min}) was determined by only including the 55,000 largest stress ranges, equal to the number of trucks in the load sequence. This implies that only the major cycle of each truck passage was included. The stress range below which the damage for AW FAT 80 is 1% is given for comparison ($\Delta S_{1\%}$). In Fig. 9, short samples of the stress-time variations of the critical (TT) sections are shown. The order of the truck passages was generated randomly once but was kept the same for all bridges.

Regarding extreme traffic events, the maximum stresses in Table 3 should be increased to account for simultaneous trucks and transverse positions of traffic. The maximum stresses thus become 413, 230, 320 and 371 MPa in the order of bridge number. In Bridge 4, however, a section adjacent to the damage-critical section experienced a higher maximum stress of 383 MPa (including extreme traffic events).

Fig. 10 shows stress range versus stress ratio and mean stress (S_m) relationships for the critical (TT) sections. It is evident that high stress ratios are dominant. In Bridge 1, for instance, all the stress ratios lie above 0.5. It can also be seen that a clear relationship exists between the stress ranges and mean stresses, i.e. fluctuating mean stress. At the mid-span of Bridge 1, all the stress cycles have a minimum stress equal to the stress from self-weight. The relationship is therefore exactly

$$S_m = k\Delta S + S_0 \quad (1)$$

with $k = 0.5$ and $S_0 = S_{self}$. Moreover, k remains at 0.5 in all sections of Bridge 1. However, for the multi-span bridges, especially Bridge 3, which has exceptionally short spans, the stress range – mean stress (ΔS-S_m) relationship is less exact, k is always less than 0.5 and it varies along the bridge sections.

4.5.1. Bridge sections involving compressive stresses, (TC) and (CC)

Bridges 3 and 4 were the only bridges where sections involving compressive stresses required HFMI treatment (i.e. damage factor $D_{AW,opt} > 1.0$). Fig. 11 shows the mean stress versus stress range relationship for these sections. In addition, lines corresponding to maximum and minimum stress equal to zero are shown, forming a triangle. Stress cycles inside the triangle are in tension-compression, cycles above the triangle are in tension-tension and cycles below the triangle are in compression-compression. For the (TC) section of Bridge 3, top flange stresses are also included; they contained higher overall mean stresses than the bottom flange but with the same damage factor ($D_{AW,opt}$). The top flange damage factors ($D_{AW,opt}$) in all the other bridges remained below 1.0.

Firstly, it is observed that the mean stresses in the (TC) sections are fairly constant. These sections are situated in transition regions near internal supports where k changes sign from positive in the spans to negative at the internal supports. Moreover, the stress ranges and mean stresses in the (TC) and (CC) sections are significantly lower than in the (TT) sections, see Table 4.

The important question regarding the (TC) sections is whether the compressive stresses are of a significant magnitude to constitute a risk of relaxing the HFMI-induced residual stresses in a way that is detrimental to fatigue life. To answer this question, Table 4 provides some characteristic quantities for the sections with the largest tensile and compressive stress.

The largest tensile stress experienced in any of the (TC) sections in Bridge 3 was +125 MPa and occurred in the top flange. In this location, the most compressive stress was −38 MPa. The most compressive stress experienced in any of the (TC) sections in Bridge 3 occurred in the same section but in the bottom flange and included the maximum and minimum stresses of +45 and −118 MPa. In Bridge 4, the (TC) section experiencing the largest tensile stress contained +155 and −1 MPa, whereas the section with the most compressive stress contained +4 and −130 MPa. Assuming that the effects of extreme traffic events which were simulated for the critical (TT) sections are also valid for the (TC) sections, the most compressive stresses would be −135 and −152 MPa in the (TC) sections of Bridges 3 and 4, respectively. The most compressive stress in any section that would require HFMI treatment occurred in a (CC) section in Bridge 3 and was −243 MPa, including extreme events.

Table 3
Characterising quantities for the critical (TT) sections in the HFMI-treated state, η = 1.56. Stresses are nominal (MPa).

Bridge	Section	L_s	R_{avg}	R_{max}	R'	S_{self}	S_{min}	S_{max}	ΔS_{min}	ΔS_{max}	$\Delta S_{1\%}$	ΔS_{eq5}	$\Delta S_{eq5,9}$
1	16.0 m	55,000	0.76	0.88	0.51	192	192	375	25	183	38	82	81
2	92.5 m	55,000	0.70	0.84	0.39	102	83	211	18	128	28	53	59
3	5.0 m	55,000	0.65	0.85	0.31	107	90	294	31	204	35	72	73
4	42.6 m	55,000	0.72	0.86	0.41	174	139	337	27	198	39	85	84

L_s – number of cycles in one load sequence (set equal to the number of trucks).
R_{avg} – average stress ratio in the load sequence.
R_{max} – highest stress ratio in the load sequence.
R' – stress ratio of the largest stress range in the load sequence.
S_{self} – stress from self-weight.
S_{min} – lowest stress valley in the load sequence including self-weight and traffic load.
S_{max} – highest stress peak in the load sequence including self-weight and traffic load.
ΔS_{min} – smallest stress range in the load sequence.
ΔS_{max} – largest stress range in the load sequence.
$\Delta S_{1\%}$ – stress range below which the damage for AW FAT 80 is 1%.
ΔS_{eq5} – single-slope (m = 5) equivalent stress range.
$\Delta S_{eq5,9}$ – double-slope (m = 5 & 9) equivalent stress range assuming FAT 140.

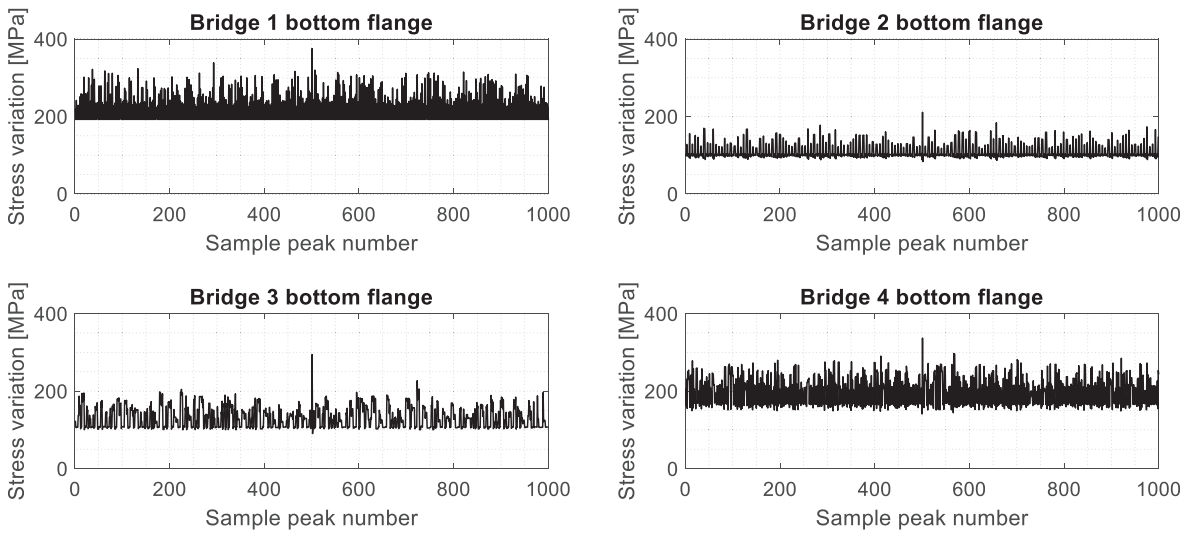

Fig. 9. Nominal stress variations from measured traffic in the critical (TT) sections in the HFMI-treated state, $\eta = 1.56$.

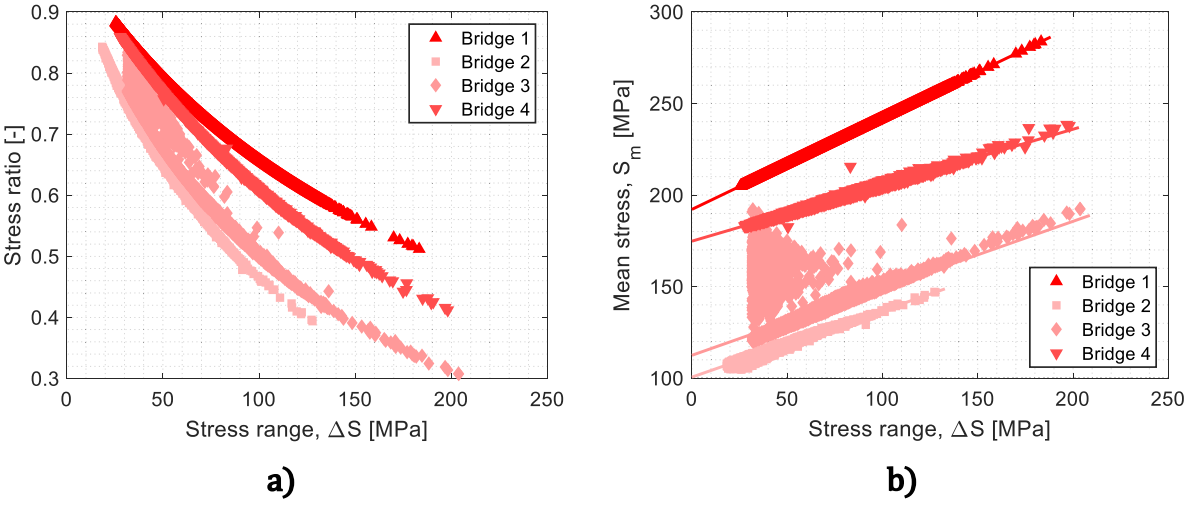

Fig. 10. Stress range versus stress ratio (a) and mean stress (b) for the damage-critical (TT) sections in the HFMI-treated state, $\eta = 1.56$.

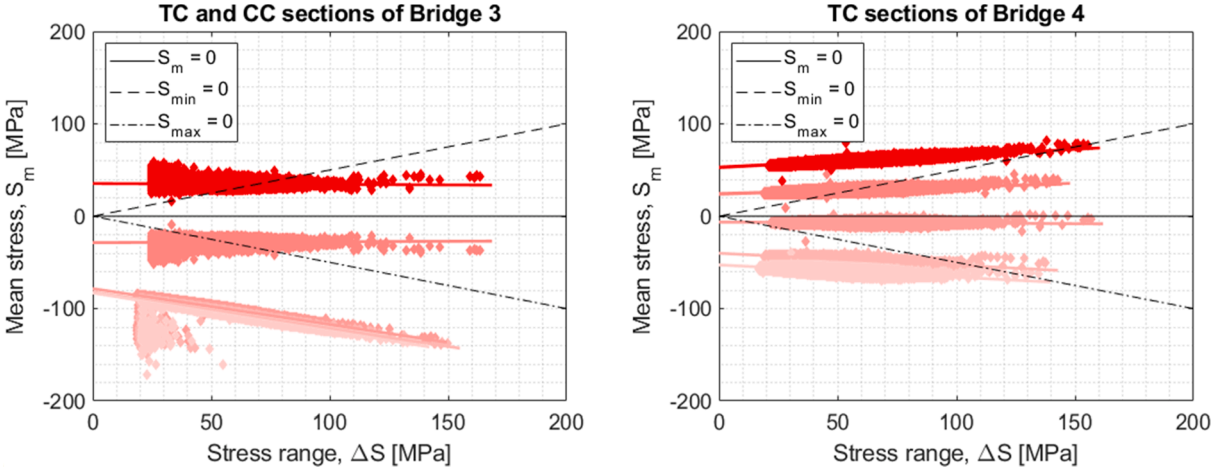

Fig. 11. Stress range versus mean stress for the (TC) and (CC) sections in the HFMI-treated state, $\eta = 1.56$.

Table 4
Characterising quantities for (TC) and (CC) sections in the HFMI-treated state, containing the largest tensile or compressive stresses, η = 1.56. Stresses are nominal (MPa).

Bridge	Category	Section	L_s	S_{self}	S_{min}	S_{max}	ΔS_{min}	ΔS_{max}	ΔS_{eq5}	$\Delta S_{eq5,9}$
3	(CC)	13.8 m	55,000	−82	−213	−63	20	150	59	64
3	(TC)	15.5 m (bot)	55,000	−25	−118	45	25	164	57	62
3	(TC)	15.5 m (top)	55,000	32	−38	125	25	164	57	62
4	(TC)	32.3 m	55,000	−54	−130	4	17	135	55	61
4	(TC)	35.6 m	55,000	52	−1	155	21	156	66	69

4.6. Evaluation of HFMI application

4.6.1. Relaxation of beneficial residual stresses

With respect to tensile overloads, the examination of available fatigue tests in the state-of-the-art review revealed that the fatigue strength of HFMI-treated specimens conformed to the IIW recommendations [38], even when nominal tensile stresses up to the yield stress were present. Regardless of this, if the IIW [38] limit for maximum tensile stress of $0.8f_y$ is respected, minimum yield stresses of 517, 288, 400 and 479 MPa would be required in the order of bridge number, for the stresses elevated by $\eta = 1.56$.

Of all the bridge sections requiring HFMI treatment, compressive stresses only occurred in Bridges 3 and 4. In relation to the yield stresses derived above from the IIW tensile stress limitation, the compressive stresses would be approximately $-0.30f_y$ in the (TC) sections of both bridges in combination with stress ratios of $R = -2.6$ and $R = -32.5$ for Bridges 3 and 4, respectively. In the (CC) section of Bridge 3, the stresses which were all compressive would reach $-0.61f_y$, with stress ratios of $R > 1$. These magnitudes of compressive stress in combination with the very low overall mean stresses would be regarded as safe, based on the state-of-the-art review with respect to conforming with the IIW fatigue strengths. For instance, it was shown in the state-of-the-art review that the case where the least compressive preload was allowed to achieve conformity with the IIW was for longitudinal attachments with preloads of $-0.46f_y$ prior to CA $R = -1$ loading [33]. Moreover, Mikkola and Remes [50] suggested a similar limit of $-0.6f_y$ for VA loading under $R = -1$. Only in the (CC) sections of Bridge 3 would such large compressive stresses occur, but, since the stresses in these sections are fully in compression and the stress ranges relatively low, no fatigue damage of any significance would occur in any case.

It is apparent that the potentially detrimental effect of residual stress relaxation due to compressive stresses is counteracted by stress cycles with low mean stresses. In no section in the four studied bridges did high compressive stresses appear in association with load cycles with high stress ranges and positive mean stress. As a result, the compressive stresses pose no detrimental effect that requires additional attention in the fatigue assessment of the studied bridges.

4.6.2. Damage assessment including mean stress

The remaining questions were how to include the mean stress effect in the assessment of damage factors for HFMI-treated welds (D_{HFMI}) and whether the inclusion of the mean stress effect would alter the location of the damage-critical sections compared with D_{AW}. To include the mean stress effect, the IIW suggested to reduce the expected increase in fatigue strength due to HFMI treatment to account for different mean stresses and stress ratios. This is referred as the R-penalty because it is based on different stress ratios. The fatigue strength of FAT 140 was chosen at low mean stress ($R < 0.15$) based on the assumption that the yield stress of the optimised HFMI-treated bridges would be in the range of $355 \leq f_y < 550$ MPa. This interval gives an increase of five FAT classes; from FAT 80 to 140, see [38]. Since the bridges included some cycles with very high stress ratios, the current IIW method was extrapolated to cover this by further increasing the penalty for every 0.12 increase in stress ratio, see Table 5. It should be noted that Mikkola et al. [61] have already verified a four FAT class penalty for the interval $0.52 < R \leq 0.7$. For the highest stress ratio intervals, fatigue strengths lower than the AW case are presumed. This may seem odd, but due to the lack of experimental data, an extrapolation of the method is the most justified and probably conservative. In this method, the *SN* curve was bi-linear with slopes 5 and 9 transitioning at 10 million cycles without any fatigue limit.

Table 5
An adaptation of the stepwise stress ratio penalty method of the IIW [38].

Stress ratio, R	FAT class reduction	Comment
$R \leq 0.15$ and $R > 1.00$	No reduction (FAT 140)	IIW modified to include (CC) sections
$0.15 < R \leq 0.28$	Reduction by one class (FAT 125)	IIW not modified
$0.28 < R \leq 0.40$	Reduction by two classes (FAT 112)	IIW not modified
$0.40 < R \leq 0.52$	Reduction by three classes (FAT 100)	IIW not modified
$0.52 < R \leq 0.64$	Reduction by four classes (FAT 90)	Extrapolation
$0.64 < R \leq 0.76$	Reduction by five classes (FAT 80)	Extrapolation
$0.76 < R \leq 0.88$	Reduction by six classes (FAT 71)	Extrapolation
$0.88 < R \leq 1.00$	Reduction by seven classes (FAT 63)	Extrapolation

Fig. 12 shows the calculated damage factors and indicates the sections containing compressive stresses. The *R*-penalty method resulted in damage factors (D_{HFMI}) that were similar to the values for AW joints ($D_{AW,opt}$, see Fig. 8) for Bridges 2 and 3 but significantly higher than those for Bridges 1 and 4. This suggests that for $\eta = 1.56$, the method predicts no benefit from HFMI treatment or even a negative effect for the bridges with the highest mean stresses. The same observation was made if the penalties were limited to a four fatigue class reduction (FAT 90) for stress ratios $0.52 < R \leq 1.00$. The reason for the observed negative effect of HFMI treatment stems from the difference in the *SN* slope where the shallow HFMI curve may be situated below the AW, see also [62,63].

Furthermore, the method predicted the same location of maximum damage factors (D_{HFMI}) as was predicted for AW joints (D_{AW}), where mean stress was not accounted for. For Bridge 4, this location changed only one metre. This is fortunate, as it allows for simpler methods for identifying the critical sections in design or assessment situations.

Moreover, the damage factors near internal supports where compressive stresses are present were just fractions of the damage at the critical sections because of the low mean stresses. In Bridge 4, two sections containing compressive stresses had somewhat higher damage factors, but the compressive stresses were very low at these locations, as shown in Table 4, section location 35.6 m. This shows that even a possible decrement in fatigue strength due to residual stress relaxation from compressive stresses would not be a critical design aspect in bridges.

4.6.3. Permissible η-values

Since the damage factors with the *R*-penalty method were unacceptably high from a design point of view, a final study was performed investigating permissible η-values as a function of material strength and whether the HFMI treatment is performed in a workshop or on site. The

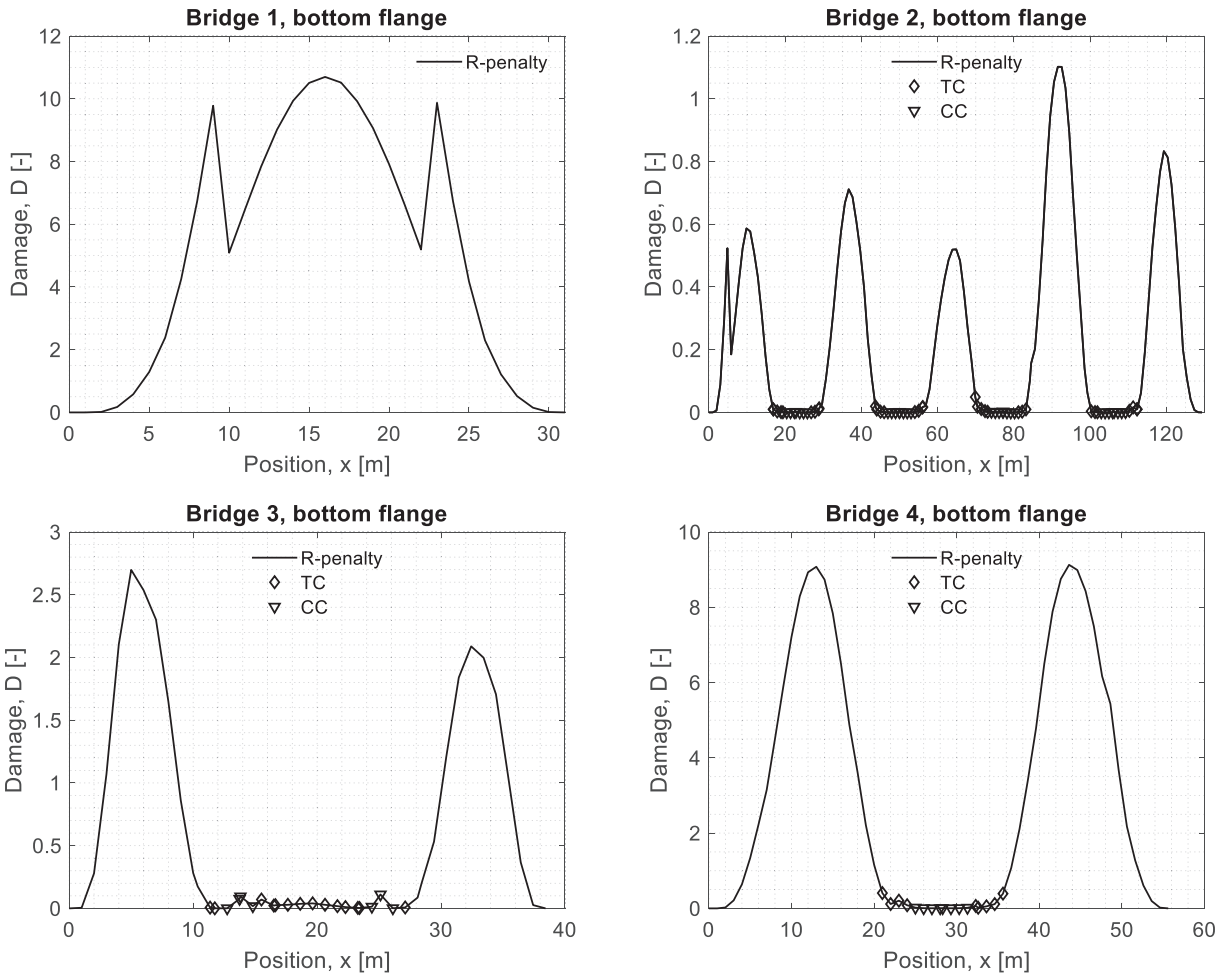

Fig. 12. HFMI damage factors for stresses from measured traffic elevated by $\eta = 1.56$ ($\gamma_{Mf} = 1.35$ and $\gamma_{Ff} = 1.0$). The R-penalty method calculated with FAT 140.

η-values can essentially be viewed as permissible factors by which the moment of inertia can be divided, representing a measurement of material saving compared with the original bridge designs. In order to obtain fair and representative permissible η-values, the criterion of $D_{HFMI} = D_{AW,orig}$ was chosen. The effect of material strength was considered indirectly by utilising various FAT classes (125, 140, 160 and 180) as the basic strength at low mean stress ($R \leq 0.15$). The IIW [38] provides intervals of yield stresses which correspond to these FAT classes; < 355 MPa (FAT 125), < 550 MPa (FAT 140), < 750 MPa (FAT 160) and < 950 MPa (FAT 180). To investigate the effect of HFMI treatment on site, it was presumed that the self-weight stresses could be set at zero in the calculations, resulting in stress ratios close to zero. Although this approach requires verification in the future, this is regarded as a reasonable assumption. Discussions and studies on this

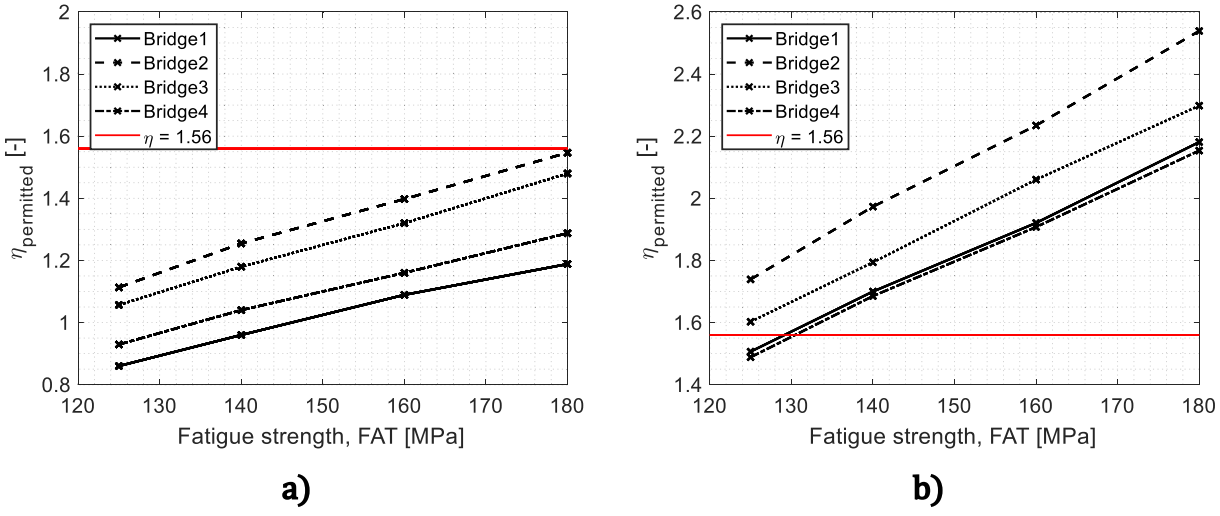

Fig. 13. Permitted η-values ($D_{HFMI} = D_{AW,orig}$) (a) including self-weight and (b) without self-weight.

subject are available in [32,49,58,64,65,66,67,68,69].

Fig. 13 shows the permissible η-values, either with (a) or without self-weight stresses (b). It can be seen that, if treatment is performed in a workshop, before the application of self-weight, the bridges would mostly not cope with the stresses elevated by $\eta = 1.56$ during their design lifetimes, see Fig. 13a. However, values of $1.0 < \eta < 1.56$ could still be possible. As seen in Fig. 13b without self-weight (treatment on site), the HFMI-treated joints in all the bridges would cope with very high η-values, but the longitudinal flange-to-web welds would become governing (i.e. $\eta = 1.56$).

5. Discussion

Some observations from the state-of-the-art review were a cause of doubt related to the fatigue strength of HFMI-treated weldments under variable amplitude loading. For instance, some studies observed real damage sums of very low values, whereas others showed values higher than 1.0. No clear connections could be made to the cause of these discrepancies, apart from the fact that different types of weldment were used. Furthermore, most of the reviewed articles used theoretical stress range spectra which are probably not relevant for bridge applications with HFMI treatment. Apart from producing the same damage, a theoretical stress range spectrum would also need to produce a correct ratio of equivalent stress range to maximum stress range and the correct magnitude of overloads. Further research is needed on spectrum shape representation for bridges subjected to HFMI treatment.

One of the objectives of this paper was to assess the maximum stresses in bridges from a residual stress relaxation aspect. Several uncertainties, which could alter the obtained results to some degree, are associated with the implemented approach. For instance, in the calculation of self-weight stresses, the effect of shrinkage of the concrete deck was neglected which, apart from higher mean stresses, would also have resulted in higher maximum stresses. Higher maximum stresses could also have been produced if real dynamic effects had been considered. The 55,000 measured trucks included in this study were measured over a total of 87 days, or, rather, about seven days per measurement site. This period is naturally not long enough to capture the extremely heavy trucks which may exist in Sweden.

In the Monte Carlo simulations where the stochastic events were simulated for 100 times the lifetimes of the bridges, the traffic intensity of 50,000 vehicle a year was used. For higher intensities, the likelihood of more extreme events that cause higher maximum stresses also increases. The large number of Monte Carlo simulations was therefore chosen to be on the safe side and cover cases with high-intensity traffic. A conservative percentage increase in the stress ranges was therefore obtained for the case-study bridges. It should be noted that bridges which are designed for higher traffic intensities are obviously also designed to experience lower stresses on average. It was therefore assumed that extreme events in high-intensity-traffic bridges would not cause higher absolute stresses than those presented in this paper. Another influencing factor in the simulations was the travel direction of the trucks which can alter the results somewhat for asymmetrical bridges. In this study, however, only one direction was investigated since the asymmetry was fairly small (see Fig. 2, Bridges 2 and 3). As a whole, more sophisticated methods can be justified for implementation in future research, but, as a starting point, the current work is considered accurate enough for the intended purpose.

Determining the relevant elevation of stresses in bridges which have been optimised with HFMI treatment was a challenging task, but a rationale was presented for finding a universal, maximum possible elevation of the stresses by a factor $\eta = 1.56$. A fatigue life prediction method (R-penalty) to include the mean stress effect was tested for HFMI-treated welds. It showed that HFMI treatment with regular steel grades is not sufficient for $\eta = 1.56$ in any of the bridges. Although more accurate methods such as fracture mechanics-based calculations could have been justified for this investigation, they are usually associated with uncertainties related to input parameters which would have changed the focus of this paper. In this case, it was more interesting to study the overall effects of HFMI; specifically, whether the critical bridge locations would change compared with AW bridges.

Since none of the variable amplitude studies in the literature review implemented the high mean stresses that exist in composite concrete and steel bridges, the R-penalty method could not be verified experimentally. This justifies the need for future experimental investigations. At a later stage in this research work, the stress range spectrum of Bridge 1 was used in a VA fatigue-testing programme with cycle-by-cycle random loading of HFMI-treated non-load-carrying transverse attachment specimens made of S460 steel (to be published). The testing of other joint types and material strengths under similar load conditions would be welcomed.

6. Conclusions

In this paper, the in-service stresses of composite steel and concrete road bridges in Sweden were investigated with the emphasis on the application of high-frequency mechanical impact treatment. Specifically, it was of interest to quantify the magnitude of mean and maximum stresses, as well as assessing the type of stress spectra and the risks of overloads. Four case-study bridges were studied in conjunction with a state-of-the-art review of relevant studies in the field of HFMI treatment. The following conclusions are drawn:

- The effect of overloads varies depending on the type of weldment and whether the load causes compression or tension at the weld toe. Compressive preloads prior to fatigue testing resulted in a decrement in fatigue strength at considerably lower load levels than tensile ones. The current compressive nominal stress limitation provided by the IIW of 45% of the yield stress is restricted to $R = -1$ applications and, as a result, it does not provide guidance on the effect of compressive preloads prior to higher mean stress fatigue loading. However, none of the preload studies achieved a fatigue strength less than that recommended by the IIW for nominal preloads of $-0.46f_y \leq S_{prel} \leq 1.0f_y$.
- Many of the reviewed studies including longitudinal attachment joints pointed towards a significant detrimental effect by variable amplitude loading (VA) on the fatigue strength of HFMI-treated joints. In spite of this, they conformed to the IIW fatigue strength recommendations. There is little evidence supporting the hypothesis that all types of joint would exhibit the same fatigue strength decrement under VA loading. Several of the studies including the VA loading of transverse attachments joints even revealed higher fatigue strength compared with constant amplitude loading.
- The largest in-service nominal stresses are tensile, with magnitudes between 40 and 70% of the yield stress in the damage-critical locations of conventional bridges. At these locations, the self-weight stresses constitute 30–50% of the maximum stresses. The ratio of equivalent stress ranges to the maximum stress ranges in the damage-critical spectra varies between 0.3 and 0.4, indicating spectra with predominantly low stress ranges with a few stress ranges of very high magnitudes. No theoretical distribution could be fitted to the stress range spectra. Compared with the Fatigue Load Model 3 of the Eurocode, the maximum stresses generated by in-service traffic are 2.3–2.4 times higher.
- A method to include the effect of mean stress in the fatigue life prediction of HFMI-treated joints was investigated and it showed that the damage-critical bridge sections remained at the same locations as in the AW bridges. It was also clear that fatigue damage is much more dominant in the span regions compared with the internal supports, partly due to the difference in mean stress. The difference in performing HFMI treatment on the site of construction, after the application of the self-weight, compared with workshop treatment

was obvious from the damage calculations which indicated substantially better performance when treating on site.
- When it came to the danger of relaxing the beneficial residual stresses, it was shown that compressive stresses are benign, as they are sufficiently low in magnitude and occur in locations with low and constant mean stresses and relatively low stress ranges. It is therefore thought that only tensile stress peaks require attention in the choice of material strength.

Declaration of Competing Interest

The authors declare that they have no known competing financial interests or personal relationships that could have appeared to influence the work reported in this paper.

Acknowledgements

This work has been partly supported by the Norwegian Public Road Administration in the project "Application of Post-weld Treatment for Lightweight Steel Bridges", partly by Vinnova in the project "LifeExt" (2017-02670) and partly by Formas (243-2014-638).

References

[1] Yıldırım HC, Remes H, Nussbaumer A. Fatigue properties of as-welded and post-weld-treated high-strength steel joints: the influence of constant and variable amplitude loads. Int J Fatigue 2020;138. https://doi.org/10.1016/j.ijfatigue.2020.105687.
[2] Carlsson F. Modelling of Traffic Loads on Bridges Based on Measurements of Real Traffic Loads in Sweden. Structural Engineering, Lund University, Lund, Sweden; 2006.
[3] Enright B. Simulation of Traffic Loading on Highway Bridges. Dublin Institute of Technology; 2010.
[4] Maddah N. Fatigue life assessment of roadway bridges based on actual traffic loads. École Polytechnique Fédérale de Lausanne 2013.
[5] Mostafa A. Calibration of Fatigue Design Factors and Fatigue Life Reliability of Steel Highway Bridges Using WIM Databases; 2015.
[6] Chen W, Xu J, Yan B, Wang Z. Fatigue load model for highway bridges in heavily loaded areas of China. Adv Steel Constr 2015;11(3):322–33.
[7] Baptista P, Alexandre C. Multiaxial and variable amplitude fatigue in steel bridges. École Polytechnique Fédérale de Lausanne 2016.
[8] Nilsson M. Secondary strain in web stiffeners in steel and composite bridges. Luleå tekniska universitet 2012.
[9] Öst M. Fatigue Study of the Vårby Bridge. Luleå tekniska universitet 2013.
[10] Saberi MR, Rahai AR, Sanayei M, Vogel RM. Bridge fatigue service-life estimation using operational strain measurements. J Bridge Eng 2016;21(5):04016005. https://doi.org/10.1061/(ASCE)BE.1943-5592.0000860.
[11] Saad T, Fu CC, Zhao G, Xu C. Development of a fatigue life assessment model for pairing fatigue damage prognoses with bridge management systems. IntechOpen 2018.
[12] Tilly GP, Nunn DE. Variable Amplitude Fatigue in Relation to Highway Bridges. Proceedings of the Institution of Mechanical Engineers 1980;194(1):259–67. https://doi.org/10.1243/PIME_PROC_1980_194_031_02.
[13] Fisher JW, Mertz DR, Zhong A. Steel bridge members under variable amplitude, long life fatigue loading, Final report, September 1983. 85p.
[14] Li ZX, Chan THT, Ko JM. Fatigue damage model for bridge under traffic loading: application made to Tsing Ma Bridge. Theor Appl Fract Mech 2001;35(1):81–91. https://doi.org/10.1016/S0167-8442(00)00051-3.
[15] Kwon K, Frangopol DM. Bridge fatigue reliability assessment using probability density functions of equivalent stress range based on field monitoring data. Int J Fatigue 2010;32(8):1221–32. https://doi.org/10.1016/j.ijfatigue.2010.01.002.
[16] Fisher JW, Roy S. Fatigue of steel bridge infrastructure. Struct Infrastruct Eng 2011;7(7–8):457–75. https://doi.org/10.1080/15732479.2010.493304.
[17] Adasooriya D. Fatigue reliability assessment of ageing railway truss bridges: Rationality of probabilistic stress-life approach. Case Stud Struct Eng 2016;6:1–10. https://doi.org/10.1016/j.csse.2016.04.002.
[18] Baptista C, Reis A, Nussbaumer A. Probabilistic S-N curves for constant and variable amplitude. Int J Fatigue 2017;101:312–27. https://doi.org/10.1016/j.ijfatigue.2017.01.022.
[19] Roy S, Fisher JW. Modified AASHTO design S – N curves for post-weld treated welded details. Bridge Struct 2006;2(4):207–22. https://doi.org/10.1080/15732480601103630.
[20] Dürr A. "Zur Ermüdungsfestigkeit von Schweißkonstruktionen aus höherfesten Baustählen bei Anwendung. von UIT-Nachbehandlung"; 2007.
[21] Fisher JW, Roy S. Fatigue damage in steel bridges and extending their life. Adv Steel Constr 2015;11(3):250–68.
[22] Gölz L, Breunig S, Kuhlmann U. Sustainable steel and composite bridges through increased lifetime by fatigue treatment. IOP Conf. Ser.: Mater. Sci. Eng., vol. 615, p. 012117, Oct. 2019, doi: 10.1088/1757-899X/615/1/012117.
[23] Walbridge S. Fatigue Analysis of Peended Bridge Welds under Realistic Service Loading Conditions Including Periodic Overload Events," Don't Mess with Stuctural Engineers; 2009. pp. 2214–2223.
[24] Ghahremani K, Walbridge S. Fatigue testing and analysis of peened highway bridge welds under in-service variable amplitude loading conditions. Int J Fatigue 2011;33(3):300–12. https://doi.org/10.1016/j.ijfatigue.2010.09.004.
[25] Tai MM, Miki PC. Improvement effects of fatigue strength by burr grinding and hammer peening under variable amplitude loading. Weld World 2012;56(7–8):109–17. https://doi.org/10.1007/BF03321370.
[26] Miki C, Tai M. Fatigue strength improvement of out-of-plane welded joints of steel girder under variable amplitude loading. Weld World 2013;57(6):823–40. https://doi.org/10.1007/s40194-013-0076-9.
[27] Ghahremani K, Walbridge S, Topper T. High cycle fatigue behaviour of impact treated welds under variable amplitude loading conditions. Int J Fatigue 2015;81:128–42. https://doi.org/10.1016/j.ijfatigue.2015.07.022.
[28] Mikkola E, Remes H, Marquis G. A finite element study on residual stress stability and fatigue damage in high-frequency mechanical impact (HFMI)-treated welded joint. Int J Fatigue 94(Part 1): 2017; 16–29, doi: 10.1016/j.ijfatigue.2016.09.009.
[29] Dalaei K, Karlsson B, Svensson L-E. Stability of shot peening induced residual stresses and their influence on fatigue lifetime. Mater Sci Eng, A 2011;528(3):1008–15. https://doi.org/10.1016/j.msea.2010.09.050.
[30] Shimanuki H, Tanaka M. Application of UIT to Suppress Fatigue Cracks of Welded Structures; 2015.
[31] Ummenhofer T, et al. REFRESH–extension of the fatigue life of existing and new welded steel structures (Lebensdauerverlängerung bestehender und neuer geschweißter Stahlkonstruktionen). Düsseldorf, Germany: Forschungsvereinigung Stahlanwendung e.V. (FOSTA); 2010.
[32] Deguchi T, et al. Fatigue strength improvement for ship structures by Ultrasonic Peening. J Mar Sci Technol 2012;17(3):360–9. https://doi.org/10.1007/s00773-012-0172-3.
[33] Ishikawa T, Shimizu M, Tomo H, Kawano H, Yamada K. Effect of compression overload on fatigue strength improved by ICR treatment. Int J Steel Struct 2013;13(1):175–81. https://doi.org/10.1007/s13296-013-1016-7.
[34] Martinez L, Haagensen PJ. Life Extension of Class F and Class F2 Details Using Ultrasonic Peening. International Institute of Welding; 2006. pp. 1–9.
[35] Eurocode 3. Design of steel structures - Part 1-9: Fatigue. European Committee for Standardization; 2005.
[36] Okawa T, Shimanuki H, Funatsu Y, Nose T, Sumi Y. Effect of preload and stress ratio on fatigue strength of welded joints improved by ultrasonic impact treatment. Weld World 2013;57(2):235–41.
[37] Polezhayeva H, Howarth D, Kumar M, Ahmad B, Fitzpatrick ME. The effect of compressive fatigue loads on fatigue strength of non-load carrying specimens subjected to ultrasonic impact treatment. Weld World 2015;59(5):713–21. https://doi.org/10.1007/s40194-015-0247-y.
[38] Marquis GB, Barsoum Z. IIW Recommendations for the HFMI Treatment - For Improving the Fatigue Strength of Welded Joints. Singapore: Springer Singapore; 2016.
[39] Leitner M, Ottersböck M, Pußwald S, Remes H. Fatigue strength of welded and high frequency mechanical impact (HFMI) post-treated steel joints under constant and variable amplitude loading. Eng Struct 2018;163:215–23. https://doi.org/10.1016/j.engstruct.2018.02.041.
[40] Huo L, Wang D, Zhang Y. Investigation of the fatigue behaviour of the welded joints treated by TIG dressing and ultrasonic peening under variable-amplitude load. Int J Fatigue 2005;27(1):95–101. https://doi.org/10.1016/j.ijfatigue.2004.05.009.
[41] Leitner M, Gerstbrein S, Ottersböck MJ, Stoschka M. Fatigue strength of HFMI-treated high-strength steel joints under constant and variable amplitude block loading. Procedia Eng 2015;101:251–8. https://doi.org/10.1016/j.proeng.2015.02.036.
[42] Marquis G, Björk T. Variable amplitude fatigue strength of improved HSS welds. International Institute of Welding. IIW Document XIII-2224-08; 2008.
[43] Yildirim HC, Marquis GB. A round robin study of high-frequency mechanical impact (HFMI)-treated welded joints subjected to variable amplitude loading. Weld World 2013; 437–447. doi: 10.1007/s40194-013-0045-3.
[44] Martinez L, Barsoum Z, Paradowska A. State-of-the-Art: Fatigue Life Extension of Offshore Installations; 2012. pp. 9–20. doi: 10.1115/OMAE2012-83044.
[45] Berg J, Stranghoener N, Kern A, Hoevel M. Variable amplitude fatigue tests at high frequency hammer peened welded ultra high strength steel S1100. Procedia Struct Integrity 2016;2:3554–61. https://doi.org/10.1016/j.prostr.2016.06.443.
[46] Yıldırım HC, Marquis G, Sonsino CM. Lightweight Potential of Welded High-strength Steel Joints from S700 Under Constant and Variable Amplitude Loading by High-frequency Mechanical Impact (HFMI) Treatment. Procedia Eng 2015;101:467–75. https://doi.org/10.1016/j.proeng.2015.02.056.
[47] Marquis G. Failure modes and fatigue strength of improved HSS welds. Eng Fract Mech 2010;77(11):2051–62.
[48] Nykänen T, Mettänen H, Björk T, Ahola A. Fatigue assessment of welded joints under variable amplitude loading using a novel notch stress approach. Int J Fatigue 2017. https://doi.org/10.1016/j.ijfatigue.2016.12.031.
[49] Mikkola E, Doré M, Marquis G, Khurshid M. Fatigue assessment of high-frequency mechanical impact (HFMI)-treated welded joints subjected to high mean stresses and spectrum loading. Fatigue Fract Engng Mater Struct 2015. https://doi.org/10.1111/ffe.12296.
[50] Mikkola E, Remes H. Allowable stresses in high-frequency mechanical impact (HFMI)-treated joints subjected to variable amplitude loading. Weld World 2016:1–14. https://doi.org/10.1007/s40194-016-0400-2.

[51] Eurocode 1. Actions on structures - Part 2: Traffic loads on bridges. European Committee for Standardization; 2003.
[52] Eurocode 3. Design of steel structures - Part 2: Steel bridges. European Committee for Standardization; 2006.
[53] Carlsson F. Utredning av ekvivalent skadefaktor för utmattningsanalyser av stålbroar, baserad på mätningar av verkliga fordonslaster i Sverige. Structural Engineering, Lund University, Lund, Sweden, TVBK-3062; 2011.
[54] ASTM E1049-85 (2017). Standard practices for cycle counting in fatigue analysis. West Conshohocken (PA): ASTM International; 2011, DOI: 10.1520/E1049-85R17.
[55] Hobbacher AF. Recommendations for Fatigue Design of Welded Joints and Components (IIW document IIW-2259-15). 2nd ed. Switzerland: Springer International Publishing; 2016.
[56] Massey Jr FJ. The Kolmogorov-Smirnov test for goodness of fit. J Am Stat Assoc 1951;46(253):68–78.
[57] Lilliefors HW. On the Kolmogorov-Smirnov test for normality with mean and variance unknown. J Am Stat Assoc 1967;62(318):399–402.
[58] Ghahremani K. Predicting the Effectiveness of Post-Weld Treatments Applied under Load; 2010.
[59] Albrecht P, Rubeiz C. Variable Amplitude Load Fatigue, Task A-Literature Review. Volume III-Variable-amplitude Fatigue Behavior. Federal Highway Administration, McLean, Va., FHwA-RD-87-061; 1990.
[60] Shams-Hakimi P. Performance of high-frequency mechanical impact treatment for bridge application; 2017.
[61] Mikkola E, Doré M, Khurshid M. Fatigue strength of HFMI treated structures under high R-ratio and variable amplitude loading. Procedia Eng 2013;66:161–70. https://doi.org/10.1016/j.proeng.2013.12.071.
[62] Kuhlmann U, Breunig S, Ummenhofer T, Weidner P. Entwicklung einer DASt-Richtlinie für höherfrequente Hämmerverfahren: Zusammenfassung der durchgeführten Untersuchungen und Vorschlag eines DASt-Richtlinien-Entwurfs. Stahlbau Oct. 2018;87(10):967–83. https://doi.org/10.1002/stab.201800021.
[63] Breunig S. Bewertung der Ermüdungsfestigkeit von Schweißnähten und ihrer Nachbehandlung im Brückenbau. Dissertation, in Vorbereitung.
[64] Fisher JW, Sullivan MD, Pense AW. Improving fatigue strength and repairing fatigue damage; Dec. 1974.
[65] Maddox SJ. Fatigue of steel fillet welds hammer peened under load. Doc. IIW-1387, Welding in the World 1998;41:343–9.
[66] Walbridge S, Nussbaumer A. Benefits of post-weld treatment to improve tubular bridge fatigue performance. In: IABSE Symposium Report, vol. 93; 2007. p. 26–33.
[67] Maddox SJ, Doré MJ, Smith SD. A case study of the use of ultrasonic peening for upgrading a welded steel structure. Weld World 2011;55(9–10):56–67.
[68] Zhao X, Wang D, Huo L. Analysis of the S-N curves of welded joints enhanced by ultrasonic peening treatment. Mater Des 2011;32(1):88–96. https://doi.org/10.1016/j.matdes.2010.06.030.
[69] Mori T, Shimanuki H, Tanaka MM. Effect of UIT on fatigue strength of web-gusset welded joints considering service condition of steel structures. Weld World 2012;56(9–10):141–9.